CHEMISTRY
A EUROPEAN JOURNAL

DOI: 10.1002/chem.200501415

Electronic Origin for Enhanced Nonlinear Optical Response of Complexes from Tetraalkylammonium Halide and Carbon Tetrabromide: Electrostatic Potentials of Intermolecular Donor–Acceptor Dyads

Wendan Cheng,* Juan Shen, Dongsheng Wu, Xiaodong Li, Youzhao Lan, Feifei Li, Shuping Huang, Hao Zhang, and Yajing Gong[a]

Abstract: Electronic origin for nonresonant enhancement of nonlinear optical response in the complexes formed from tetraalkylammonium halide and carbon tetrabromide is provided in view of electrostatic potentials of intermolecular donor (halide ion)–acceptor (CBr_4). The calculated electrostatic potentials of donor–acceptor range from -4.83 to -7.70 kcal mol^{-1} and show a decreasing order of $[Et_4Cl^-\cdots Br] > [Et_4Br^-\cdots Br] \cong [Et_4I^-\cdots Br] > [Bu_4Br^-\cdots Br]$. The calculated second-order susceptibilities of solid complexes are in an increasing order of $[NEt_4Cl{\cdot}CBr_4] < [NEt_4Br{\cdot}CBr_4] \cong [NEt_4I{\cdot}CBr_4] < [NBu_4Br{\cdot}CBr_4{\cdot}C_3H_6O]$. It has been shown that the donor/acceptor dyads make the exclusive contribution to nonlinear optical response. A large size of halide or tetraalkylammonium ion results in a small electrostatic potential and large nonlinear optical response in these charge-transfer complexes. It indicates that a small supermolecular interaction will create a large nonlinear optical response, and it gives a clue to design the molecular complexes with large non-linear optical susceptibility.

Keywords: charge transfer · electrostatic interactions · hyperpolarizability · molecular cluster · nonlinear optics

Introduction

The rational design of noncentrosymmetry solids to be applied to second-order nonlinear optics has attracted a lot of attention,[1–8] due to the fact that second-order nonlinear optical (NLO) materials are key to the future photonics technology. Evans, Lin, et al.[2] employed an asymmetric bridging ligand to exploit the intrinsic lack of inversion symmetry to obtain an interesting array of noncentrosymmetric Cd and Zn complexes for NLO applications. Desiraju and co-workers[4] also attempted the ice-related assembly of asymmetrical tetraphenylmethane moieties to synthesize noncentrosymmetry solids, and Hoskins and Robson[5] developed an approach, not through linear, but through tetrahedral copper(I) "joints" that results in diamondoid networks with alternate tetrahedral nodes.[9] However, theoretical studies of molecular solids stayed behind experimental works in NLO properties. Calculations of NLO properties beyond the isolated chromophore level are still not very common, and most research efforts are only related to first hyperpolarizability β calculations of NLO chromophores. A clear understanding for the molecular solids at the supermolecular scale is unavailable, since the interactions governing the assembly stability depend on intermolecular distance and direction. As a result, with the knowledge of the optical properties of the individual molecule, a predication at the supermolecular level such as crystals, thin films or poled polymers has not been possible. This is due to the lack of information about the interactions among the individual molecules. In most assemblies, weak intermolecular forces like the electrostatic interactions, hydrogen bonding, dipole–dipole interactions, π-stacking and charge-transfer interactions, control the overall structure and stability of the molecular solids.[10,11] Accordingly, the subtle balance between these forces governs the NLO properties of molecular solids.[12]

[a] Prof. W. Cheng, Dr. J. Shen, Dr. D. Wu, Dr. X. Li, Dr. Y. Lan, Dr. F. Li, Dr. S. Huang, H. Zhang, Y. Gong
State Key Laboratory of Structural Chemistry
Fujian Institute of Research on the Structure of Matter
The Chinese Academy of Sciences
Fuzhou, Fujian 350002 (P.R. China)
Fax: (+86) 0591-8371-4946
E-mail: cwd@ms.fjirsm.ac.cn

Supporting information for this article is available on the WWW under http://www.chemeurj.org/ or from the author: Cartesian coordinates of all the molecular clusters are listed in Table S1, first-order hyperpolarizability components and some excited states contributing to hyperpolarizability at input energy of 0.818 eV at SOS//TDB3LYP/3-21G* level are separately listed in Table S2 and S3.

The calculations of NLO properties at supermolecular or molecular cluster scales have been reported, in which electronic structure calculations were carried out for a finite cluster of chromophores.[13–21] Calculations on the 3-methyl-4-nitropyridine-1-oxide (POM) crystal and 2-methyl-4-nitroaniline (MNA) crystal have shown that the first hyperpolarizability of the molecular clusters originates from a dominant low-energy charge-transfer excited state,[13] and molecular cluster size and arrangement make a great influence upon nonlinear optical properties.[14] Also interesting is the situation in which the calculations of NLO properties were carried out for the donor/acceptor complexes.[17,18] The calculated β of charge-transfer complex constructed by the coplanar 1,2,4,5-tetramethylbenzne and TCNE molecules has a large value, and the large β response arises from a strongly allowed transition at relatively low excitation frequency.[18] For the tetraalkylammonium halide (NR_4h)/carbon tetrabromide (CBr_4) dyad, the three-dimensional (diamondoid) network consists of donor (halide ion) and acceptor (CBr_4) nodes alternately populated to result in the effective annihilation of centers of symmetry in a good agreement with the sphalerite structural subclass. Such inherently acentric networks exhibit intensive nonlinear optical properties.[1] In this study, we will theoretically investigate size influences of the halide anions (X^-, X = Cl, Br, and I) and tetraalkylammonium cations (NR_4^+, R = Et, Bu) on the electrostatic interactions and NLO properties in terms of molecular cluster model for the $[NR_4X{\cdot}CBr_4]$ complexes. Furthermore, we will systematically discuss the NLO response from continuous charge-transfers through the network of donor/acceptor in the crystal state complexes of $[NR_4X{\cdot}CBr_4]$.

Methods and Procedures

The nature of electronic excitation state were computed by using the time-dependent density functional theory at the B3LYP/3-21G* (TDB3LYP/3-21G*) level[22–24] for the $[NEt_4X{\cdot}CBr_4]_2$ (X = Cl, Br, and I) and $[NBu_4Br{\cdot}CBr_4{\cdot}C_3H_6O]_2$ molecular clusters. The calculations were performed with the Gaussian03 program.[25] Becke′ three parameter of Lee–Yang–Parr (B3LYP) hybrid function including exact exchange and correlation functions and the standard basis sets of 3-21G* stored internally in the Gaussian 03 program were employed. More precise basis sets were required in the calculation of a small system, here, we considered the balance between the consuming resources and calculating precise of the large system in the chosen basis sets. The influence of basis set size on the hyperpolarizability β was discussed in the calculations of 2-methyl-4-nitroaniline (MNA).[14] The SCF convergence criteria of the root-mean-square (rms) density matrix and the maximum density matrix were set at 10^{-8} and 10^{-6}, respectively, in all the electronic structure calculations. The range of molecular orbitals for correlation was from orbital 103 to 530 for the $[NEt_4Cl{\cdot}CBr_4]_2$, from orbital 111 to 550 for the $[NEt_4Br{\cdot}CBr_4]_2$, from orbital 129 to 570 for the $[NEt_4I{\cdot}CBr_4]_2$, and from orbital 135 to 854 for the $[NBu_4Br{\cdot}CBr_4{\cdot}C_3H_6O]_2$ molecular clusters in the TDB3LYP/3-21G* calculations. The iterations of excited states were continued until the changes on energies of states were no more than 10^{-7} a.u. between the iterations, and then the convergences of 50 excitation states were obtained in the calculations.

NLO (nonlinear optical) responses were calculated by the sum-over-states (SOS) method derived from the standard time-dependent perturbation theory.[26,27] The Kohn–Sham Hamiltonian was uncoupled with the applied field, and electronic excited states created by the field were treated as an infinite sum over unperturbed partical-hole states. Generally, the dynamic first-order hyperpolarizability β_{ijk} is given as:[14,17]

$$\beta_{ijk}(\omega_3;\,\omega_1,\,\omega_2) = 1\,\hbar_{\mathrm{Pf}}^{-2}\sum{}_{\mathrm{mn}}\mu_{\mathrm{gn}}^{\mathrm{i}}\mu_{\mathrm{nm}}^{\mathrm{j}}\mu_{\mathrm{mg}}^{\mathrm{k}}[(\omega_{\mathrm{ng}}-\omega_3)(\omega_{\mathrm{mg}}-\omega_2)]^{-1} \quad (1)$$

The SOS perturbation theory expression for the hyperpolarizability indicated that one requires dipole moments of ground state and excited states, the transition moments from ground to excited states and from excited to excited states, and state-state transition energies. The moments and energies were obtained from the TDB3LYP/3-21G* calculations in this study. The SOS expansion was, in general, infinite, since the applied optical field mixes the molecular ground state with many excited states. For the calculation of β, we generally truncated the infinite SOS expansion to a finite one after apparent convergence of β had been reached. Here, we employed the TDB3LYP method based on 3-21G* basis sets to calculate excited state and NLO properties.

For molecular cluster model, the whole solid was reduced to a giant molecule and is treated with standard quantum chemical calculations. This model constitutes the straightforward method to include nonadditive intermolecular effects but it often suffers from huge computational costs when dealing with large molecular clusters. Moreover, the influence of the environment effects on the first hyperpolarizability of increasingly large clusters is related to shift of the low-energy absorption bands. The calculations of hyperpolarizability based on SOS method require a large number of excited state knowledge. Therefore, to balance the computational costs and reliable calculated results, we selected the molecular cluster structures from geometry of the repeat units of complex crystal, that is, the molecular clusters were within the unit cell consisting in a single crystal.[1] The molecular cluster geometries in SOS//TDB3LYP/3-21G* calculations are plotted in Figure 1. The charge-transfer complexes of tetraethylammonium salts with halide ions (such as chloride, bromide, and iodide) are a graded series of the diamondoid donor/acceptor network, in which the tetrahedral CBr_4 alternates in a regular manner with the halide at the nodes of adamantance-like cage.[1] Figure 1a shows the $[NEt_4X{\cdot}CBr_4]_2$ molecular clusters, containing four molecules, two for CBr_4 molecules and two for NEt_4X molecules. A noticeable chain of diamondoid donor/acceptor can be seen in

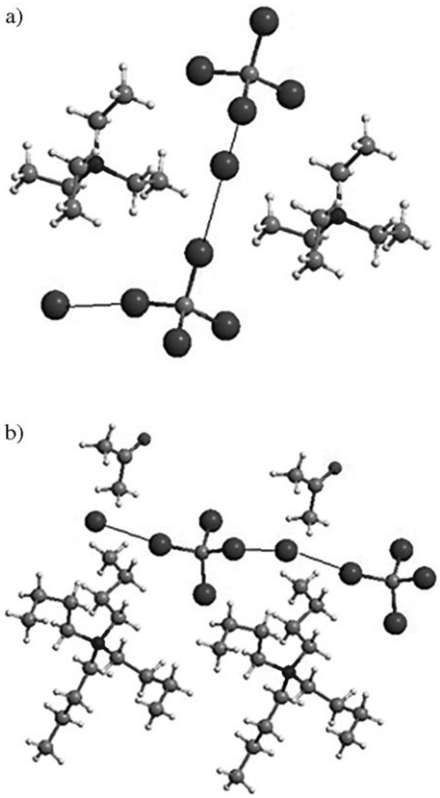

Figure 1. Configurations of molecular clusters: a) $[NEt_4X{\cdot}CBr_4]_2$ (X = Cl, Br, and I); b) $[NBu_4Br{\cdot}CBr_4{\cdot}C_3H_6O]_2$.

the structures. The halide ion (donor) and CBr_4 (acceptor) connections are shown as thin line and the NEt_4^+ counterions localize at each side of the chain. The molecular cluster $[NBu_4Br{\cdot}CBr_4{\cdot}C_3H_6O]_2$, which forms by the tetrabutylammonium bromine, carbon tetrabromide and acetone, is shown in Figure 1b. The two NBu_4^+ counterions localize at one side of the chain formed by $Br{\cdots}BrC(Br)_2Br{\cdots}Br{\cdots}BrCBr_3$, whereas the two C_3H_6O molecules localize at the other side.

Results and Discussion

Excited-state properties: Before discussing the electronic origination of first hyperpolarizability of complexes formed from halide salts and carbon tetrabromide, we need to know the excited state nature of molecular clusters. Accordingly, the transition energies, moments, and oscillator strengths of 50 excited states were calculated at the TDB3LYP/3-21G* level for the clusters $[NEt_4X{\cdot}CBr_4]_2$ (X = Cl, Br, and I) and $[NBu_4Br{\cdot}CBr_4{\cdot}C_3H_6O]_2$. The electronic excitation states with a large transition probability mostly localized in the range from 2.30 to 2.80 eV for the studied molecular clusters as listed in Table 1. Figure 2 depicts the relationships between the oscillator strengths and absorption wavelengths for the lowest 50 excited states. It is found that these complexes exhibit electronic transitions in the visible range from 440 to 550 nm (A band) and in the UV range from 290 to 330 nm (B band). The A band is sharp and mostly arises from the intermolecular charge transfers from the halide ion of NEt_4X (X = Cl, Br, and I) or NBu_4Br to CBr_4 molecule in the complexes. For example, excited state S_8 of $[NEt_4Cl{\cdot}CBr_4]_2$, $[NEt_4I{\cdot}CBr_4]_2$ and $[NBu_4Br{\cdot}CBr_4{\cdot}C_3H_6O]_2$, and S_9 of $[NEt_4Br{\cdot}CBr_4]$, which contributes to A band, is mostly due to contribution from the configuration of (HOMO−2 → LUMO+1), respectively. For all the considered species, the HOMO−2 is mostly formed from the halide ion *p* orbitals, and the LUMO+1 is formed from CBr_4 group orbitals with small mixings of halide ionic orbitals. The plots of the HOMO−2 and LUMO+1 of $[NEt_4Br{\cdot}CBr_4]_2$ molecular clusters are given in Figure 3. Remarkably, we found that these two frontier orbitals exclude the counterion contributions, and the occupied cluster orbital is mostly constructed by one Br ion orbital with small mixings of CBr_4 group orbitals and the unoccupied orbital is mostly formed from one CBr_4 group orbital with small mixings of two Br orbitals. Accordingly, the A band is assigned as the charge transfers from one halide ion (donor) of

Table 1. Calculated transition energies, moments, and oscillator strengths of important excited states.

State	*E* [eV]	Moment [D]			Oscillator strength
		x	*y*	*z*	
			$[NEt_4Cl{\cdot}CBr_4]_2$		
S_1	0.8814	0.0213	−0.0033	−0.0023	0.0000
S_8	2.6091	1.8974	−2.6963	−1.3192	0.1248
S_{12}	2.7859	−3.0656	−1.1967	−1.6445	0.1430
S_{25}	3.9640	1.7383	0.3968	−0.6675	0.0545
S_{28}	4.0739	−2.2004	−0.4923	0.6428	0.0849
S_{40}	4.3236	−1.0838	0.1972	0.4405	0.0231
			$[NEt_4Br{\cdot}CBr_4]_2$		
S_1	0.6733	0.0383	−0.0031	−0.0041	0.0000
S_9	2.4945	−2.6889	2.6094	1.0564	0.1434
S_{12}	2.6482	−2.9632	−1.8753	−1.8875	0.1593
S_{25}	3.8290	2.1818	0.6291	−0.7521	0.0831
S_{28}	3.9556	−2.3227	−0.6865	0.5566	0.0926
			$[NEt_4I{\cdot}CBr_4]_2$		
S_1	0.8908	0.0976	−0.0033	−0.0061	0.0000
S_7	2.3246	−0.3497	−0.0252	−0.1843	0.0014
S_8	2.5386	−3.9740	2.0304	0.4646	0.1938
S_9	2.6317	−2.0118	−2.9294	−2.3389	0.1806
S_{23}	3.7742	1.7302	0.4552	−0.7084	0.0530
S_{24}	3.8634	−1.9752	−0.3696	0.5023	0.0629
S_{25}	3.8801	1.4862	0.8927	−0.3459	0.0460
			$[NBu_4Br{\cdot}CBr_4{\cdot}C_3H_6O]_2$		
S_1	1.6305	0.0350	−0.0130	0.0252	0.0000
S_8	2.3089	−5.5230	1.5451	−1.9582	0.3216
S_9	2.4342	−2.5340	0.3398	−0.2458	0.0612
S_{13}	2.8557	1.4074	0.4331	−2.0309	0.0681

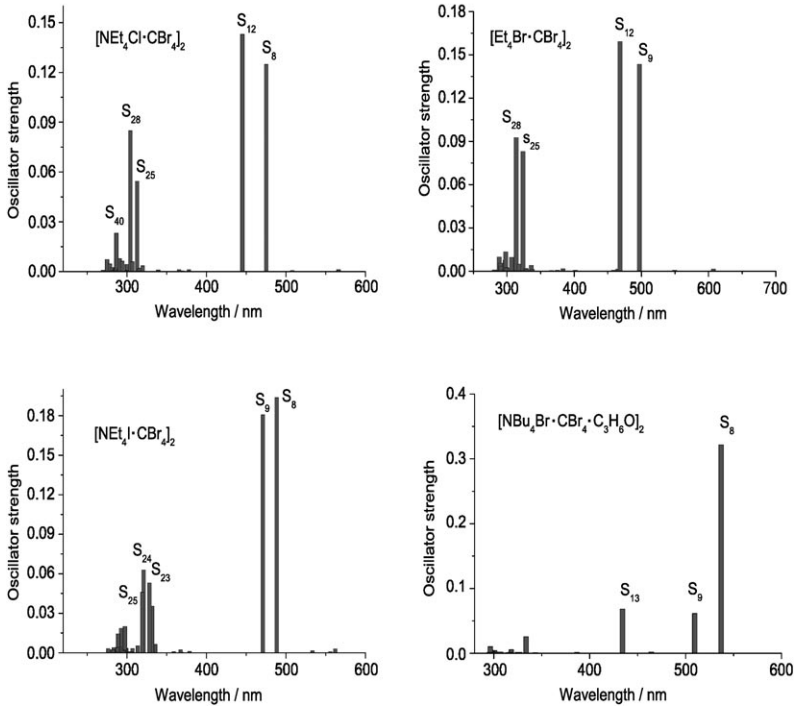

Figure 2. Calculated absorption spectra at the TDB3LYP/3-21G* level.

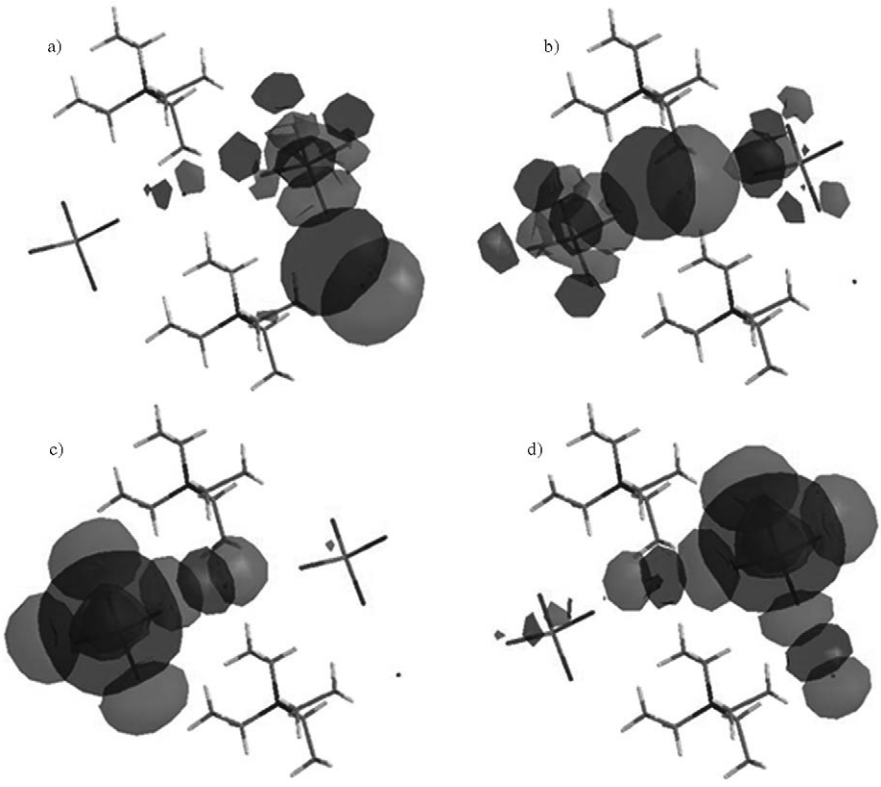

Figure 3. Calculated frontier orbitals of molecular cluster $[NEt_4Br{\cdot}CBr_4]_2$ at TDB3LYP/3-21G* level: a) HOMO−2, b) HOMO−5, c) LUMO, d) LUMO+1.

NEt_4X (X = Cl, Br, and I) to one CBr_4 molecule (acceptor). The B band, as shown in Figure 2, is broad and originates from the charge transfers within molecular cluster ($[X^-{\cdot}CBr_4]_2$). For instance, excited state 28 of $[NEt_4Br{\cdot}CBr_4]_2$ contributing to B band is mostly constructed by the configuration (HOMO−5 → LUMO+1). The occupied orbital HOMO−5 is exclusively constructed by the $[Br_3CBr{\cdots}Br{\cdots}BrCBr_3]$ cluster orbital, and the unoccupied orbital LUMO+1 is a significantly contribution from the $[Br{\cdots}BrC(Br_2)Br{\cdots}Br]$ cluster orbital, as plotted in Figure 3, respectively. The calculated absorption peak wavelength of B band is in an increasing order from Cl^- (304 nm) < Br^- (313 nm) < I^- (321 nm) in the $[NEt_4X{\cdot}CBr_4]_2$ molecular clusters. The variation trends are the same as those of the measured absorption wavelength λ_{max} [Cl^- (265 nm) < Br^- (292 nm) < I^- (345 nm)] of $[NPr_4X{\cdot}CBr_4]$ complexes.[1] However, the calculated A absorption bands have not been observed in experiment. For the $[NBu_4Br{\cdot}CBr_4{\cdot}C_3H_6O]_2$ molecular cluster, the absorption peak at the lowest energy has a red shift comparing with that of a small size counterion of NEt_4^+, as shown in Figure 2.

First-order hyperpolarizability β: For the calculations of polarizability β, we first considered how to truncate the infinite SOS expansion to a finite one. Figure 4 shows the plots of the calculated hyperpolarizabilities $\beta_{tot}(-2\omega;\omega,\omega)$[17,28] at the SOS//TDB3LYP/3-21G* level versus the number of states for the studied molecular clusters at input photon energy of $\hbar\omega = 0.818$ eV (i.e., wavelength = 1.52 μm). It is found that the curves have similar shapes, that is, the same behaviors of convergence in β_{tot} values of the $[NEt_4X{\cdot}CBr_4]_2$ (X = Cl, Br, and I) and

$[NBu_4Br{\cdot}CBr_4{\cdot}C_3H_6O]_2$ molecular clusters. These curves can be divided into two segments. The first segment formed below state 13 has a sharp variation, and the second segment formed after state 14 is smooth. For example, the calculated value of β_{tot} including 12 states is from 95 to 101% of the β_{tot} value including 50 states at SOS//TDB3LYP/3-21G* level at an input energy of 0.818 eV for all of the studied molecular clusters. In order to further check convergent behavior, we also give the plots of state-dependent hyperpolarizability $\beta_{tot}(-2\omega;\omega,\omega)$ at $\hbar\omega = 0.00$ eV (static case) for all the studied clusters. As depicted in Figure 4 the shapes of the four curves are almost the same and the convergences reach with summation over 15 states at static case for all of the studied clusters. Accordingly, it is shown from the state-dependent hyperpolarizabilities that the calculations of β are reliable for the $[NEt_4X{\cdot}CBr_4]_2$ (X = Cl, Br, and I) and $[NBu_4{\cdot}CBr_4{\cdot}C_3H_6O]_2$ molecular clusters when we truncate 50 states by using the SOS//TDB3LYP method.

The calculated frequency dependence of β_{tot} values is plotted in Figure 5 for the $[NEt_4X{\cdot}CBr_4]_2$ (X = Cl, Br, and I) and $[NBu_4{\cdot}CBr_4{\cdot}C_3H_6O]_2$ clusters, respectively. It is found that the resonant enhancements appear after input energy larger than 1.05 eV and no dispersion exists at the input photon energy less than 0.90 eV for the studied clusters. The hyperpolarizabilities of β_{tot} given above are found to be dominated by some excited charge-transfer states. Table 2 lists the important states contributing to β_{tot} at the input photon energy of 1.165 eV and the configuration components of these states (similar results at the input energy of 0.818 eV are listed in Table S3 of the Supporting Information). For example, the eighth excited state of the $[NEt_4Cl{\cdot}CBr_4]_2$ cluster has 72% contributions to the β_{tot}, and this state has the greatest component from the configuration of 0.6302 (HOMO−2 → LUMO+1). From Table 2, we find that the state making the largest contribution to the β_{tot} is created from the configuration (HOMO−2 → LUMO+1) for the studied clusters. As shown earlier, the HOMO−2 orbital receives the most contributions from orbitals of halide (Cl, Br, and I) donor; the LUMO+1 orbital has significant contributions from acceptor $[CBr_4]$ group orbital. The calculated donor orbital contributions in the HOMO−2 orbital are 64, 67, 83, and 68%, but they are only 5, 6, 4, and 7% in LUMO+1 of the $[NEt_4X{\cdot}CBr_4]_2$ (X = Cl, Br, and I) and $[NBu_4Br{\cdot}CBr_4{\cdot}C_3H_6O]_2$ clusters individually. In the same analyses, we found that the nonresonant hyperpolarizabilities at low energy region are also contributions from the dyads of halide ion and carbon tetrabromide. For example, at the input photon energy of 0.818 eV, the β_{tot} is mostly contributed from HOMO−2, HOMO−5, and LUMO, LUMO+1 orbitals. Therefore, it is clear that the intermolecular charge transfers give significant contributions to the hyperpolarizability β of the clusters studied. In the following discussion, we will prensent evidence of nonresonant enhanced NLO response in the acentric complexes formed from the tetraalkylammonium halide and carbon tetrabromide.

Table 2. Properties of states contributing to hyperpolarizability (10^{-28} cm^5 esu^{-1}) at photon energy of 1.165 eV.

Cluster	State	Configuration	TM [D][a]	β_{tot}[i]	β_{tot}	%
$[NEt_4Cl{\cdot}CBr_4]_2$	S_8	0.6302 (H−2→L+1)	3.551	2.5568	3.5807	71.4
	S_{12}	0.6435 (H−5→L)	3.679	0.8470		23.7
$[NEt_4Br{\cdot}CBr_4]_2$	S_9	0.6142 (H−2→L+1)	3.893	5.1828	6.6789	77.6
	S_{12}	0.6236 (H−5→L)	3.982	1.4314		21.4
$[NEt_4I{\cdot}CBr_4]_2$	S_7	0.6597 (H−4→L)	0.396	2.0344	6.2549	32.5
	S_8	0.5592 (H−2→L+1)	4.316	2.3092		36.9
	S_9	0.5432 (H−5→L)	1.943	1.8798		30.1
$[NBu_4Br{\cdot}CBr_4{\cdot}C_3H_6O]_2$	S_8	0.5779 (H−2→L+1)	6.060	83.0984	78.6354	106
	S_9	0.5639(H−5→L)	2.568	−3.2824		−4.2

[a] TM is transition moment from ground to excited states

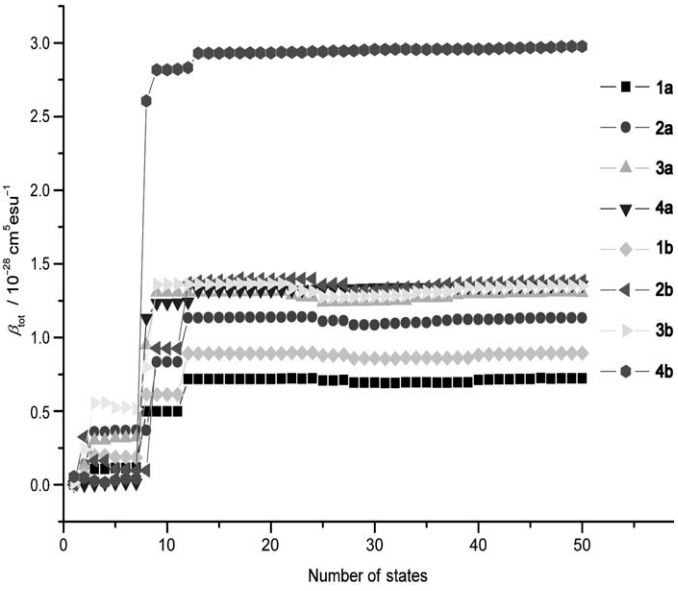

Figure 4. Calculated state-dependent hyperpolarizability β_{tot} of $[NEt_4X{\cdot}CBr_4]_2$; 1 for X = Cl, 2 for X = Br, 3 for X = I, 4 for $[NBu_4Br{\cdot}CBr_4{\cdot}C_3H_6O]_2$; a and b is at photon energy of 0.0 and 0.818 eV, respectively.

Electrostatic potentials of intermolecular donor–acceptor: The charge redistributions in the intermolecular charge-transfer complexes of $[NEt_4X{\cdot}CBr_4]$ (X = Cl, Br, and I) and $[NBu_4Br{\cdot}CBr_4{\cdot}C_3H_6O]$ form while we compare them with those found in isolated molecules of CBr_4 and tetraalklammonium halide. The basic findings using the Mulliken atomic populations are as follows: in a $[Br_3CBr{\cdots}X^-]$ complex compared with the isolated molecules of CBr_4 and $Et_4N^+X^-$, the halide ion and Br of CBr_4 lose electrons, and C gains electrons. It shows charge transfers from the Et_4N^+ X^- to CBr_4. Accordingly, the electrostatic interaction between the halide ion and $BrCBr_3$ appears in the complexes of $[X^-{\cdots}BrCBr_3]$. Here, we note that the halide ion still car-

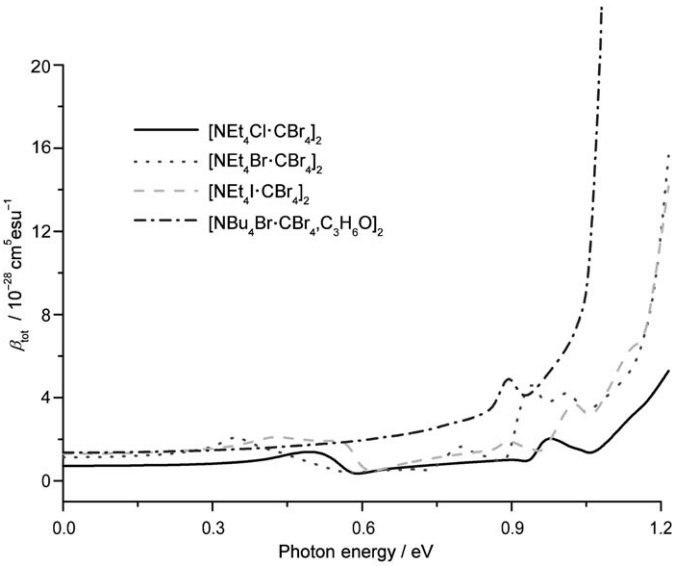

Figure 5. Calculated dynamic hyperpolarizability β_{tot} at SOS//TDB3LYP/3-21G* level.

ries negative charge in spite of the loos of some charge in the complexes. The attraction energy of intermolecular donor–acceptor with negative Q^- and positive Q^+ charges, and separated by distance R, is obtained from Coulomb's law.[29] The calculated atomic charges of halide ion donor and bromine acceptor in the CBr_4 based on the TDB3LYP/3-21G* level, in which the Br acceptor has close contact to the halide ion,[1] are listed in Table 3. It is found that the calculated attraction electrostatic potentials of intermolecular donor–acceptor range from -4.83 to -7.69 kcal mol^{-1}, and show the variation trends of the absolute values in the order of $[Et_4Cl^-\cdots Br] > [Et_4Br^-\cdots Br] \cong [Et_4I^-\cdots Br] > [Bu_4Br^-\cdots Br]$. This finding corresponds to the red shift of absorption peaks in an increasing order of $[NEt_4Cl{\cdot}CBr_4]_2 < [NEt_4Br{\cdot}CBr_4]_2 \cong [NEt_4I{\cdot}CBr_4]_2 < [NBu_4Br^-{\cdot}CBr_4]_2$ (see Figure 2). Furthermore, the dynamic first-order hyperpolarizabilities plotted in Figure 5 increase in the order of $[NEt_4Cl{\cdot}CBr_4]_2 < [NEt_4Br{\cdot}CBr_4]_2 \cong [NEt_4I{\cdot}CBr_4]_2 < [NBu_4Br^-{\cdot}CBr_4]_2$. For example, the calculated hyperpolarizabilities β_{tot} range from 0.89×10^{-28} to 2.98×10^{-28} cm^{5}esu^{-1} at an input photon energy of 0.818 eV for all of the species considered. From the variation trends of electronic potentials, transition energies (absorption wavelengths), and first-order hyperpolarizabilities among the studies clusters, we found that the $[NBu_4Br{\cdot}CBr_4{\cdot}C_3H_6O]_2$ has the smallest electronic potential and transition energy, and the largest first-order hyperpolarizability. This is due to the fact that a small electrostatic potential (absolute value) creates small transition energy, and the small transition energy results in a large first-order hyperpolarizability according to Equation (1). The fact that a small electrostatic potential results in a large NLO response was described in the study of supermolecular interaction in 2-methyl-4-ntroaniline (MNA) crystal, where a small supermolecular interaction of MNA dimer leads to a large NLO response.[14] The $[NEt_4Cl{\cdot}CBr_4]_2$ cluster with the smallest size of Cl^- ion has the largest attraction energy and smallest first-hyperpolarizability, and it can be ascribed to the strongest electrostatic interaction between the halide donor and carbon tetrabromide acceptor among the studied molecular clusters. Accordingly, the first-order hyperpolarizability is in inverse proportion to the intermolecular attractive energy in the $[NR_4X{\cdot}CBr_4]_2$ molecular clusters. Moreover, the electrostatic interaction of attractive energy is also in inverse proportion to the distance between two atoms. Noted here, the contact distance of intermolecular donor–acceptor of $I^-\cdots BrCBr_3$ is larger than that of $Br^-\cdots BrCBr_3$; however, the latter charges Q_hQ_{Br} (-0.0498 e^2) are smaller than the former (-0.0519 e^2). Coulomb's law[29] shows that the attractive energy is direct related to the charge and inverse to the distance between two species. These contradictory contributions to attractive energy give almost equal attraction energy between the $[NEt_4X\cdots CBr_4]$ (X = Br, I) complexes. Hence, the first-order hyperpolarizability of $[NEt_4Br\cdots CBr_4]_2$ is almost the same as that of $[NEt_4I\cdots CBr_4]_2$. Now, we discuss the origin of small attractive energy and large hyperpolarizability of $[NBu_4Br{\cdot}CBr_4{\cdot}C_3H_6O]_2$ molecular cluster. As shown by Kochi and co-workers,[1] a large size of NBu_4^+ counterion fills in the cavity of diamondoid network and results in a large intermolecular distance of ($Br_3CBr\cdots Br^-$) and a small C-Br$\cdots$Br$^-$ angle in the $[NBu_4Br{\cdot}CBr_4{\cdot}C_3H_6O]$ complex. When we compared the Mulliken atomic populations between the $Br\cdots Br^-$ in the $[NEt_4Br{\cdot}CBr_4]$ and that in the $[NBu_4Br{\cdot}CBr_4{\cdot}C_3H_6O]_2$ clusters, as shown in Table 3, respectively, we found that the average charges $Q_{Br}Q_{Br^-}$ are almost the same between these two clusters. Accordingly, the small attractive energy is ascribed to large distance of $Br\cdots Br^-$, and large hyperpolarizability is originated from small electrostatic interaction for the $[NBu_4Br{\cdot}CBr_4{\cdot}C_3H_6O]_2$ cluster.

Table 3. Attraction energies of intermolecular donor–acceptor for $[CBr_4{\cdot}halide]_2$ complexes.

Cluster	Q_h [e]	Q_{Br} [e]	R [Å]	E [kcal mol^{-1}]	β_{tot} [10^{-28} cm^{5}esu^{-1}][a]
$NEt_4Cl{\cdot}BrCBr_3$	-0.7177	0.0997	3.090	-7.6902	0.8946
$NEt_4Br{\cdot}BrCBr_3$	-0.7244	0.0688	3.154	-5.2476	1.3832
$NEt_4I{\cdot}BrCBr_3$	-0.6551	0.0793	3.298	-5.2310	1.3501
$NBu_4Br{\cdot}BrCBr_3$	-0.6222	0.0764	3.266	-4.8335	2.9758
	-0.7146	0.0706	3.253	-5.1504	

[a] In order to describe the first hyperpolarizability of nonresonant enhancement, here the β_{tot} is given at input photon energy of 0.818 eV.

Nonlinear optical susceptibilities of crystalline donor/acceptor assemblies: Average macroscopic second-order susceptibility $\chi^{(2)}$ of the assembly was computed in terms of the relation with microscopic first-order hyperpolarizability by $\chi^{(2)}(\omega) = NL\ ||\beta(\omega)||$.[14,30] The norm value $||\beta||$ is invariant to any rotation, that is, it is independent from the orientation of coordination axis of molecular cluster, and it represents an average of different components β. N and L represent separately cluster density numbers and local field correction factor at radiation frequency ω.[31] The obtained sus-

ceptibility $\chi^{(2)}$ and the parameters of N, L, and $||\beta||$ to be used to compute the susceptibility are listed in Table 4. In order to make comparisons, we have also listed the calculated β_{vec}.[17,28] Here, we note the different quantity of definition of β. If their values are close among the β_{vec}, β_{tot} and $||\beta||$ values, the charge transfer is unidirectional and parallel to the molecular dipole moment. Our calculated results show that the largest components contributing to β_{vec}, β_{tot}, and $||\beta||$ are β_{iii} ($i=x$ or y) components for the $[NEt_4X{\cdot}CBr_4]_2$ clusters (X = Cl, Br, and I) and β_{iij} ($i \neq j$) for the $[NBu_4Br{\cdot}CBr_4{\cdot}C_3H_6O]_2$ cluster (see Table 3, Supporting Information). From the values in Tables 3 and 4, however, we found that the estimated assembly susceptibility $\chi^{(2)}$ obtained whether from β_{tot} or from $||\beta||$ value varies in an increasing order of $[NEt_4Cl{\cdot}CBr_4] < [NEt_4Br{\cdot}CBr_4] \cong [NEt_4I{\cdot}CBr_4] < [NBu_4Br{\cdot}CBr_4{\cdot}C_3H_6O]$. Accordingly, a large second-order susceptibility of crystalline donor/acceptor assembly comes from a large first-order hyperpolarizability of molecular cluster, and the latter is originated from a small electrostatic interaction of intermolecular donor–acceptor.

Table 4. Calculated crystal second-order susceptibilities from molecular clusters $[NR_4X{\cdot}CBr_4]_2$ at nonresonant frequency of $\omega = 0.818\ eV\hbar^{-1}$.[a]

Species	β_{vec}	$\|\|\beta\|\|$	L	N	$\|\|\chi^{(2)}\|\|$
$[NEt_4Cl{\cdot}CBr_4]_2$	0.8811	0.8762	1.1107	1.2730	1.2389
$[NEt_4Br{\cdot}CBr_4]_2$	1.3755	1.2792	1.1477	1.2277	1.8024
$[NEt_4I{\cdot}CBr_4]_2$	1.3299	1.3922	1.1749	1.1274	1.8441
$[NBu_4Br{\cdot}CBr_4{\cdot}C_3H_6O]_2$	2.1347	4.0171	1.0601	0.7061	3.0069

[a] Unit: β for 10^{-28} $cm^5\,esu^{-1}$, N for 10^{21} cm^{-3}, $\chi^{(2)}$ for 10^{-7} esu.

Conclusion

Our time-dependent DFT study of the nature of excitation state and the electronic origin of nonlinear optical response for the assemblies of $[NEt_4X{\cdot}CBr_4]$ and $[NBu_4{\cdot}CBr_4{\cdot}C_3H_6O]$ complexes, where X = Cl, Br, and I, discloses the fact that the intermolecular donor (halide)/acceptor (bromine) dyads make the exclusive contribution to nonlinear optical response, and a weak electrostatic potential of intermolecular donor–acceptor creates a large second-order susceptibility. The calculated electrostatic potentials of intermolecular donor–acceptor range from -4.83 to $-7.70\ kcal\,mol^{-1}$ and show a decreasing order of $[Et_4Cl^{-}{\cdots}Br] > [Et_4Br^{-}{\cdots}Br] \cong [Et_4I^{-}{\cdots}Br] > [Bu_4Br^{-}{\cdots}Br]$, and the calculated second-order susceptibilities of solid complexes are in an increasing order of $[NEt_4Cl{\cdot}CBr_4] < [NEt_4Br{\cdot}CBr_4] \cong [NEt_4I{\cdot}CBr_4] < [NBu_4Br{\cdot}CBr_4{\cdot}C_3H_6O]$ at the SOS//TDB3LYP/3-21G* level. A large cavity of network constructing by halide donor and carbon bromide acceptor results in a weak electrostatic interaction (charge-transfer interaction) for the halide and carbon tetrabromide [1:1] complexes. Our findings indicate that weak charge-transfers or weak supermolecular interactions will make large nonlinear optical responses in acentric complexes, and it gives a clue to design the molecular complexes with large nonlinear optical susceptibility.

Acknowledgements

This investigation was based on work supported by the National Natural Science Foundation of China under projects 20373073 and 90201015, the National Basic Research Program of China No.2004CB720605, the Science Foundation of the Fujian Province (E0210028), and the Foundation of State Key Laboratory of Structural Chemistry (030060).

[1] S. V. Lindeman, J. Hecht, J. K. Kochi, *J. Am. Chem. Soc.* **2003**, *125*, 11597.
[2] a) O. R. Evans, W. Lin, *Acc. Chem. Res.* **2002**, *35*, 511; b) W. Lin, L. Ma, O. R. Evans, *Chem. Commun.* **2000**, 2263; c) O. R. Evans, Z. Wang, R.-G. Xiong, B. M. Foxman, W. Lin, *Inorg. Chem.* **1999**, *38*, 2969; d) O. R. Evans, R.-G. Xiong, Z. Wang, G. K. Wong, W. Lin, *Angew. Chem.* **1999**, *111*, 557; *Angew. Chem. Int. Ed.* **1999**, *38*, 536.
[3] O. R. Evans, W. Lin, *Chem. Mater.* **2001**, *13*, 2705; O. R. Evans, W. Lin, *Chem. Mater.* **2001**, *13*, 3009.
[4] R. Thaimattam, C. V. K. Sharma, A. Clearfield, G. R. Desiraju, *Cryst. Growth Des.* **2001**, *1*, 103.
[5] a) B. F. Hoskins, R. Robson, *J. Am. Chem. Soc.* **1990**, *112*, 1546; b) B. F. Hoskins, R. Robson, *J. Am. Chem. Soc.* **1989**, *111*, 5962.
[6] W. Lin, W. Lin, G. K. Wong, T. J. Marks, *J. Am. Chem. Soc.* **1996**, *118*, 8034.
[7] T. J. Marks, M. A. Ratner, *Angew. Chem.* **1995**, *107*, 167; *Angew. Chem. Int. Ed. Engl.* **1995**, *34*, 155.
[8] H. E. Katz, W. L. Wilson, G. Scheller, *J. Am. Chem. Soc.* **1994**, *116*, 6636.
[9] a) D. S. Reddy, D. C. Craig, G. R. Desiraju, *Chem. Commun.* **1994**, 1457; b) D. S. Reddy, D. C. Craig, A. D. Rae, G. R. Desiraju, *Chem. Commun.* **1993**, 1737.
[10] a) A. J. Stone, *The theory of intermolecular forces*, Oxford University Press, **1996**; b) H. Ratajczak, W. J. Orvill-Thomas, *Molecular interactions*, Wiley, **1980**.
[11] a) D. Bragal, L. Maini, M. Polito, F. Grepioni, *Struct. Bonding (Berlin)* **2004**, *111*, 1; b) L. Brammer, *Chem. Soc. Rev.* **2004**, *33*, 476.
[12] D. S. Chemla, J. Zyss, *Nonlinear optical properties of organic molecules and crystals*, Academic Press, **1987**.
[13] M. Guillaume, E. Botek, B. Champagne, F. Castet, L. Ducasse, *J. Chem. Phys.* **2004**, *121*, 7390.
[14] W.-D. Cheng, D.-S. Wu, H. Zhang, X.-D. Li, D.-G. Chen, Y.-Z. Lang, Y.-C. Zhang, Y.-J. Gong, *J. Phys. Chem. B* **2004**, *108*, 12658.
[15] L. Jensen, P.-O. Strand, A. Osted, J. Kongsted, K. V. Mikklsen, *J. Chem. Phys.* **2002**, *116*, 4001.
[16] G. Maroulisa, *J. Chem. Phys.* **2000**, *113*, 1813.
[17] D. R. Kanis, M. A. Ratner, T. J. Marks, *Chem. Rev.* **1994**, *94*, 195.
[18] a) S. DeBella, I. L. Fragala, M. A. Ratner, T. J. Marks, *J. Am. Chem. Soc.* **1993**, *115*, 682; b) S. DeBella, M. A. Ratner, T. J. Marks, *J. Am. Chem. Soc.* **1992**, *114*, 5842.
[19] T. Yasukawa, T. Kimura, M. Uda, *Chem. Phys. Lett.* **1990**, *169*, 219.
[20] K. V. Mikkelsen, M. A. Ratner, *J. Phys. Chem.* **1989**, *93*, 1759.
[21] J. Zyss, G. Berthier, *J. Chem. Phys.* **1982**, *77*, 3635.
[22] M. E. Casida, C. Jamorski, K. C. Casida, D. R. Salahub, *J. Chem. Phys.* **1988**, *108*, 4439.
[23] R. Bauernschmitt, R. Ahlrichs, *Chem. Phys. Lett.* **1996**, *256*, 454.
[24] R. E. Stratman, G. E. Scuseria, M. J. Frisch, *J. Chem. Phys.* **1998**, *109*, 8218.
[25] Gaussian 03, Revision C02, M. J. Frisch, G. W. Trucks, H. B. Schlegel, G. E. Scuseria, M. A. Robb, J. R. Cheeseman, J. A. Montgomery, Jr., T. Vreven, K. N. Kudin, J. C. Burant, J. M. Millam, S. S. Iyengar, J. Tomasi, V. Barone, B. Mennucci, M. Cossi, G. Scalmani, N. Rega, G. A. Petersson, H. Nakatsuji, M. Hada, M. Ehara, K. Toyota, R. Fukuda, J. Hasegawa, M. Ishida, T. Nakajima, Y. Honda, O. Kitao, H. Nakai, M. Klene, X. Li, J. E. Knox, H. P. Hratchian,

J. B. Cross, C. Adamo, J. Jaramillo, R. Gomperts, R. E. Stratmann, O. Yazyev, A. J. Austin, R. Cammi, C. Pomelli, J. W. Ochterski, P. Y. Ayala, K. Morokuma, G. A. Voth, P. Salvador, J. J. Dannenberg, V. G. Zakrzewski, S. Dapprich, A. D. Daniels, M. C. Strain, O. Farkas, D. K. Malick, A. D. Rabuck, K. Raghavachari, J. B. Foresman, J. V. Ortiz, Q. Cui, A. G. Baboul, S. Clifford, J. Cioslowski, B. B. Stefanov, G. Liu, A. Liashenko, P. Piskorz, I. Komaromi, R. L. Martin, D. J. Fox, T. Keith, M. A. Al-Laham, C. Y. Peng, A. Nanayakkara, M. Challacombe, P. M. W. Gill, B. Johnson, W. Chen, M. W. Wong, C. Gonzalez, J. A. Pople, Gaussian, Inc., Pittsburgh, PA, **2003**.

[26] J. F. Ward, *Rev. Mod. Phys.* **1965**, *37*, 1.

[27] B. J. Orr, J. F. Ward, *Mol. Phys.* **1971**, 20.

[28] The definitions of $\beta_{tot}=(\Sigma\beta_i^2)^{1/2}$,(and) $\beta_{vec}=\Sigma\mu_i\beta_i/|\mu|$, and $\beta_i=\beta_{iii}+{}^1/_3\Sigma(\beta_{ijj}+\beta_{jij}+\beta_{jji})$, here, i and j run over the molecular Cartesian direction x, y, and z, and μ is ground-state molecular dipole moment, in summation $i \neq j$.

[29] Coulomb's law, $E=(Q^+Q^-)/(4\pi\varepsilon_0 R)$, the calculations may be simplified if $4\pi\varepsilon_0=1.112650\times10^{-10}J^{-1}C^2m^{-1}$ and electronic charge $e=1.60219\times10^{-19}$ C. To multiply by 2.30711×10^{-18} J, when we computed the attraction energy using Mulliken atomic charges and distances in angstrom Å. To convert from J to erg, multiply by 10^7, and from erg to kcal mol^{-1} multiply by 1.43942×10^{13}.

[30] J. Zyss, in *Nonlinear Optics* (Ed.: S. Miyata), Elsevier, Amsterdam, **1992**, pp. 33; The definition of $||\beta||^2=\beta_{xxx}^2+\beta_{yyy}^2+\beta_{zzz}^2+3(\beta_{xyy}^2+\beta_{yxx}^2+\beta_{xzz}^2+\beta_{zxx}^2+\beta_{yzz}^2+\beta_{zyy}^2)+6\beta_{xyz}^2$.

[31] a) N is defined as the product of mass density and Avogadro's constant divided by the molar mass. The local field correction factor is calculated from the $L=f_{2\omega}f_\omega^2$, and $f_\omega=[n(\omega)^2+2]/3$ with the assumption of Lorentz–Lorenz local field. Here, $n^2=1+4\pi\chi^{(1)}$ and $\chi^{(1)}=N\alpha/(1-4\pi N\alpha/3)$. The α is first-order polarizability and $\chi^{(1)}$ is first-order susceptibility; b) R. W. Boy, *Nonlinear Optics*, Academic Press, San Diego, CA, **1992**, pp. 148.

Received: November 15, 2005
Revised: February 21, 2006
Published online: June 22, 2006

